Journal of Organometallic Chemistry, 402 (1991) 289–312
Elsevier Sequoia S.A., Lausanne
JOM 21299

Intramolecularly coordinated arylmagnesium compounds: effects on the Schlenk equilibrium

Peter R. Markies, Rinke M. Altink, Alan Villena, Otto S. Akkerman, Friedrich Bickelhaupt *

Scheikundig Laboratorium, Vrije Universiteit, De Boelelaan 1083, 1081 HV Amsterdam (Netherlands)

Wilberth J.J. Smeets and Anthony L. Spek

Vakgroep Algemene Chemie, Afdeling Kristal- en Structuurchemie, University of Utrecht, Padualaan 8, 3584 CH Utrecht (Netherlands)

(Received July 23rd, 1990)

Abstract

A series of phenylmagnesium bromides (**1**, **3–8**) with *ortho*-substituents capable of forming intramolecular coordinative bonds along with the corresponding diarylmagnesium compounds (**1a**, **3a–6a**, **8a**) have been synthesized. The thermodynamic parameters ΔH_s and ΔS_s for the Schlenk equilibria ($2\ ArMgBr \rightleftharpoons Ar_2Mg + MgBr_2$) have been determined by variable temperature NMR spectroscopy. Crystal structures were obtained of 5,6,8,9-tetrahydrodibenz[*d*,*g*][1,6]oxamagnesecin (**2a**) and bis(2,6-di(methoxymethyl)phenyl)magnesium (**4a**). The extent of intramolecular coordination in these compounds as determined in the solid state, is used in the discussion of the influence of substituents on the Schlenk equilibrium parameters. Unusual penta- or hexa-coordination is encountered and explained as a consequence of intramolecular coordination.

Introduction

In THF solution, a Grignard compound partially disproportionates reversibly into the corresponding diorganylmagnesium compound and magnesium bromide; this is known as the Schlenk equilibrium. In dilute solutions of phenylmagnesium bromide, both the Grignard (**1**) and diphenylmagnesium (**1a**) are monomers with tetra-coordinated magnesium atoms (Scheme 1); magnesium bromide is also monomeric, but occurs as a tetrakis-tetrahydrofuranate complex [1].

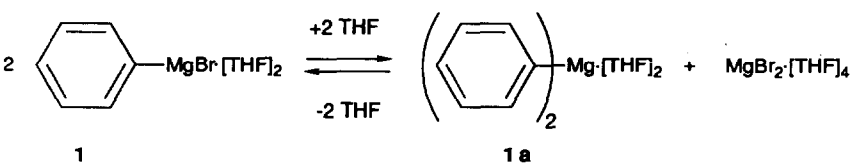

1 **1a**

Scheme 1

0022-328X/91/$03.50

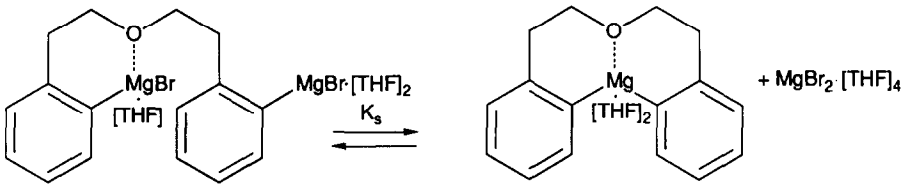

2 2a

Scheme 2

From measurements of the heats of reaction between $MgBr_2$ and Ph_2Mg in dilute THF solutions (thermochemical titration), the thermodynamic parameters of the Schlenk equilibrium ΔH_s (-11.8 kJ mol^{-1}) and ΔS_s (-50.6 J mol^{-1} K^{-1}) have been derived [2,3]. An independent determination of ΔH_s and ΔS_s by low temperature ^{1}H NMR spectroscopy yielded values of $\Delta H_s = -13.3$ kJ mol^{-1} and $\Delta S_s = -56$ kJ mol^{-1} K^{-1} [4]. Values for ΔG_s and K at room temperature ($T = 298$ K), of 3.28 kJ mol^{-1} and 0.266 respectively, can be calculated from the first set of parameters.

Substitution of the aromatic ring of **1** with groups capable of intramolecular coordination will change the equilibrium, since the complexation modes of the Grignard and the symmetrized reagent will be influenced differently. Clear indications of this effect were found in our studies of the di-Grignard reagent 1,5-bis(2-bromomagnesiophenyl)-3-oxapentane (**2**, Scheme 2) [5,6]: the position of the Schlenk equilibrium (in THF solution) was found to lie completely on the side of the diarylmagnesium species **2a**. In this special case, the position of the equilibrium could be determined from association measurements (stationary isothermal distillation), since, in contrast to the normal situation (Scheme 1), the position of the equilibrium determines the number of particles in solution. A stabilization of the (monomeric ! [5]) magnesacycle **2a** through the formation of an intramolecular coordinative bond was postulated to account for the stability of **2a** relative to that of **2**, resulting in a decrease of free energy (ΔG_s) going from left to right in Scheme 2. However, **2a** is not stabilized relative to **1a** as was concluded later from thermochemical experiments: the heat of reaction of **2a** with acetic acid is more exothermic than that of **1a** (**2a** $\Delta H_R = -199.6(3.9)$, **1a** $\Delta H_R = -190.6$ kJ mol^{-1} per Mg–C bond) [6–8].

Results and discussion

To clarify the contradictory evidence outlined above we determined the crystal structure of **2a** (Fig. 1); when crystallized from THF it appeared to be quite different from that of normal tetra-coordinated $R_2Mg \cdot L_2$ complexes. The ether oxygen of **2a** and the central magnesium atom are included in a ten-membered ring which favours formation of an intramolecular coordinative bond; surprisingly, two molecules of THF are also coordinated to the magnesium atom (a more detailed discussion of this crystal structure is given below). We assume that the coordination of magnesium of **2a** in solution is analogous to that in the solid state. A qualitative description of the influence of intramolecular coordination on the Schlenk equilibrium can thus be based on the crystal structure of **2a** and the postulated structure of **2**.

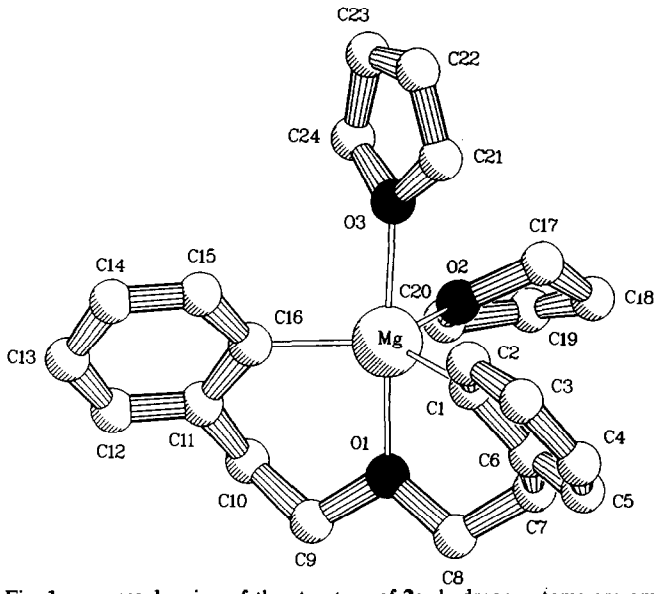

Fig. 1. PLUTON drawing of the structure of **2a**; hydrogen atoms are omitted for clarity.

Two factors can be distinguished which yield a negative value for ΔG_s and hence shift the Schlenk equilibrium to the right:

(i) In both compound **2a** and in magnesium bromide, the magnesium atoms are effectively coordinated; the crystal structures of both compounds show a total of seven Mg–O bonds (three in **2a** and four in $MgBr_2$ [9]). Coordination in **2** is probably less efficient; the two magnesiums will be tetra-coordinated and use either four molecules of THF or three molecules of THF plus an intramolecular ether oxygen to complete their coordination spheres (the latter situation is shown in Scheme 2). Therefore the number of Mg–O bonds increases by three upon conversion of **2** into **2a** and $MgBr_2$, which yields a negative value for ΔH_s and hence makes a negative contribution to ΔG_s.

(ii) As mentioned before, the conversion of a di-Grignard into the diorganylmagnesium compound and magnesium bromide (Scheme 2) is, in contrast to that for a mono-functional Grignard reagent (Scheme 1), entropically favourable in so far that the number of dissolved particles increases ($\Delta S_s > 0$); there is, on the other hand, a loss of conformational freedom as well as an increase in the number of coordinated molecules of THF, which renders any guess at the value or even the sign of ΔS_s a mere speculation.

Therefore it was desirable to obtain ΔH_s and ΔS_s experimentally, e.g. by determination of the relative amounts of ArMgBr and Ar_2Mg from:

$2\ ArMgBr \rightleftarrows Ar_2Mg + MgBr_2$; $[Ar_2Mg] = [MgBr_2]$, hence:

$$K = \frac{[Ar_2Mg]^2}{[ArMgBr]^2}$$

The value of K was determined at various temperatures and ΔH_s and ΔS_s were obtained from a plot of ln K versus $1/T$ (Van 't Hoff plot). This method was not feasible for **2** since the equilibrium appeared to lie almost completely to the side of

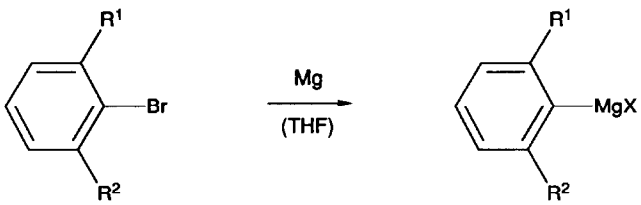

ArBr	X = Br	(X = Ar)
$R^1 = R^2 = H$	1	1a
9: $R^1 = CH_2OMe$, $R^2 = H$	3	3a
10: $R^1 = R^2 = CH_2OMe$	4	4a
11: $R^1 = CH_2CH_2OMe$, $R^2 = H$	5	5a
12: $R^1 = CH_2NMe_2$, $R^2 = H$	6	6a
13: $R^1 = R^2 = CH_2NMe_2$	7	7a
14: $R^1 = R^2 = H$; *p*-CH_2OMe	8	8a

Scheme 3

2a. In contrast, analysis of the Schlenk equilibria of **3–8** (Scheme 3) proved to be possible by variable temperature NMR spectroscopy. Compounds **3–7** were chosen as analogues of **2** because they contain one or two *ortho*-substituents which are capable of forming a five- or six-membered chelate ring, while **1** and **8** may serve as models without intramolecular coordination. Between 200 and 298 K, the exchange reaction between the Grignard and diorganylmagnesium species is slow on the NMR time scale, allowing their separate detection. Both ^1H and ^{13}C NMR spectroscopy can be used, the relative amounts of ArMgBr and Ar_2Mg being determined by integration of the appropriate NMR signals. The value of K was calculated from signals of pairs of corresponding protons or carbon atoms in ArMgBr and Ar_2Mg.

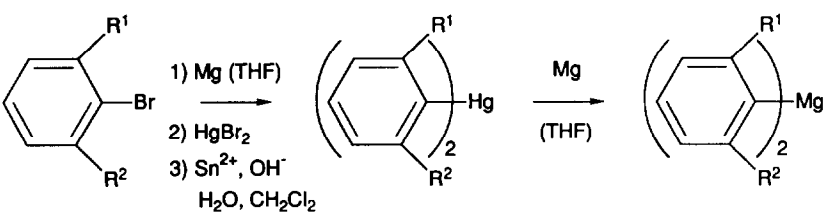

ArBr	Ar_2Hg	Ar_2Mg
$R^1 = R^2 = H$	21	1a
9: $R^1 = CH_2OMe$, $R^2 = H$	15	3a
10: $R^1 = R^2 = CH_2OMe$	16	4a
11: $R^1 = CH_2CH_2OMe$, $R^2 = H$	17	5a
12: $R^1 = CH_2NMe_2$, $R^2 = H$	18	6a
13: $R^1 = R^2 = CH_2NMe_2$	19	(7a)
14: $R^1 = R^2 = H$; *p*-CH_2OMe	20	8a

Scheme 4

Table 1

Temperatures [a] and ln K values [b] for the Schlenk equilibria: 2 $ArMgBr \rightleftharpoons Ar_2Mg + MgBr_2$

1 (^{13}C NMR)		3 (^{1}H NMR)		4 (^{1}H NMR)		5 (^{1}H NMR)		6 (^{1}H NMR)		7 (^{1}H NMR)		8 (^{13}C NMR)	
T	ln K	T	ln K	T	ln K	T	ln K	T	ln K	T	ln K	T	ln K
209.1	1.167	205.3	−2.891	207.5	−1.182	199.5	−0.387	227.4	−4.020	223.5	−2.960	203.1	2.091
214.2	0.978	210.7	−2.997	211.8	−1.025	204.2	−0.370	232.0	−3.957	228.7	−3.337	213.9	1.570
219.4	0.670	216.1	−2.875	216.1	−0.997	208.8	−0.263	234.8	−3.866	234.0	−3.761	219.3	1.360
224.5	0.421	218.3	−2.931	220.4	−0.903	213.5	−0.042	236.9	−3.895	239.3	−3.879	224.6	1.059
226.5	0.400	223.6	−2.983	224.7	−0.842	218.1	−0.431	241.3	−3.808	244.5	−4.351	230.0	0.983
229.6	0.270	225.8	−2.998	229.0	−0.780	222.8	−0.001	246.0	−3.611	249.8	−4.771	235.4	0.698
232.7	0.117	229.0	−3.015	233.3	−0.706	227.4	0.189	248.8	−3.579	255.1	−4.865	240.8	0.572
235.8	−0.061	234.4	−3.090	237.7	−0.651	232.0	0.061	253.4	−3.811	260.3	−5.316		
		236.6	−3.194			236.7	−0.096	258.1	−3.889	265.6	−5.492		
		239.8	−3.232			241.3	−0.290	261.8	−4.012	270.9	−6.285		
		245.2	−3.378			246.0	−0.503	266.4	−4.084	276.1	−6.409		
		250.6	−3.510			250.6	−0.665	271.1	−4.174	281.4	−6.670		
		256.0	−3.632			255.3	−0.844	275.7	−4.292	286.7	−6.915		
		258.1	−3.677			259.9	−1.030	281.3	−4.399				
		261.4	−3.752			264.6	−1.326	285.0	−4.470				
		266.7	−3.900			269.2	−1.468	288.7	−4.513				
		268.9	−4.005			273.9	−1.598	292.5	−4.603				
		272.1	−4.120			278.5	−1.732	296.2	−4.690				
		277.5	−4.246					301.8	−4.914				
		279.7	−4.275					306.4	−4.953				
		282.9	−4.288					311.1	−5.008				
		287.2	−4.311										
		291.5	−4.416										

[a] In kelvin. [b] The temperature range used for the calculation of ΔH_s and ΔS_s is indicated in Table 2

Table 2

Parameters ΔH_s and ΔS_s for the Schlenk equilibria: 2 $ArMgBr \rightleftharpoons Ar_2Mg + MgBr_2$

Cpd.	NMR-techn. (r value) [a]	Temp. range (K)	ΔH_s (kJ mol^{-1})	ΔS_s (J mol^{-1} K^{-1})	Grignard composition at 298 K		
					K	ArMgBr(%)	Ar_2Mg(%)
1 [b]	^{13}C (0.993)	209-236	−18.7	−79.3	0.134	73	27
3 [c]	^{1}H (0.990)	234-292	−13.7	−83.9	0.010	91	9
4	^{1}H (0.985)	208-238	+6.8	+23.0	1.061	49	51
5	^{1}H (0.993)	227-279	−20.8	−89.1	0.100	76	24
	^{1}H (0.93)	199-213	+8	+36			
6	^{1}H (0.989)	249-311	−14.1	−86.9	$8.57 \cdot 10^{-3}$	92	8
	^{1}H (0.94)	227-246	+10	+10			
7	^{1}H (0.987)	224-287	−33.9	−175.4	$6.06 \cdot 10^{-4}$	98	2
8	^{13}C (0.993)	203-241	−16.5	−64.0	0.352	63	37

[a] r: Correlation factors. [b] The literature values for **1** are calculated using a different definition for K. [c] A deviation of the ln K versus $1/T$ curve in the direction of more positive ΔH_s and ΔS_s value was observed at lower temperatures ($T < 234$ K; see Table 1).

Solutions of the Grignard compounds **1–8** were prepared by reacting the bromides (bromobenzene and **9–14**) with magnesium in THF-d_8. In order to identify the signals in the low temperature NMR spectra, they were compared with those of the pure diorganylmagnesium compounds (**1a**, **3a–6a**, and **8a**), obtained from the exchange reactions of the corresponding diorganylmercury compounds with magnesium (**15–21**; Scheme 4), measured under identical conditions. In the case of **19**, no exchange reaction took place (even at 60 °C), probably for steric reasons. Therefore, **7a** was prepared from **7** and the corresponding organolithium compound.

The results of the NMR measurements are listed in Table 1. The values for ΔH_s and ΔS_s together with the composition of the equilibrium mixture at 298 K, are presented in Table 2.

We first discuss the results for the Schlenk equilibrium of **1**, **3**, **5**, **6**, and **8**, which, according to Table 2, have comparable thermodynamic parameters: ΔH_s ranges from −14 to −21 kJ mol^{-1}; ΔS_s ranges from −64 to −87 J mol^{-1} K^{-1}, those of **1** fall approximately in the middle of this range. This close similarity can be understood on the basis of a number of simplifying assumptions:

(1) The coordination of **1** and **1a** in solution corresponds to that in the solid state, i.e. the magnesium is tetra-coordinated [1] which is also the case for structurally comparable compounds.

(2) The enthalpies of the Mg–O bonds in **1** and **1a** (and in analogous organomagnesium compounds) are equal. This assumption, which is reasonable for ArMgBr and Ar_2Mg, may seem less so for $MgBr_2$ (a stronger Lewis acid), but this is compensated by the binding of four molecules of THF which will reduce the average binding enthalpy per molecule of THF.

(3) The change in entropy upon binding a molecule of THF is approximately constant.

(4) Other changes connected with the occurrence of the Schlenk equilibrium are negligible for both enthalpy and entropy.

In our opinion these assumptions are self-evident and plausible. Of course, the crude character of these first approximations allows only semiquantitative conclu-

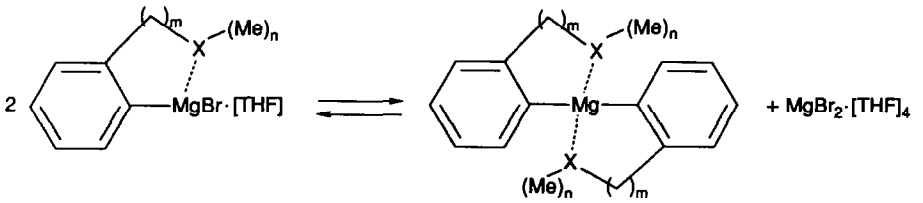

m=1; n=1; X=O : **3**
m=2; n=1; X=O : **5**
m=1; n=2; X=N : **6**

m=1; n=1; X=O : **3a**
m=2; n=1; X=O : **5a**
m=1; n=2; X=N : **6a**

Scheme 5

sions to be drawn. The reasonably consistent picture emerging may be taken as an indication of the validity of this approach.

Applied to the Schlenk equilibrium of the parent system **1** (Scheme 1), we note that the transformation 2 $PhMgBr \rightleftharpoons Ph_2Mg + MgBr_2$ has the following consequences:

(i) the number of magnesium-containing particles is constant ($\Delta N = 0$);
(ii) the number of Mg–O bonds increases by two ($\Delta(Mg–O) = +2$);
(iii) the number of bonded THF molecules increases by two ($\Delta(THF) = +2$).

The concomitant change in enthalpy ($\Delta H_s = -18.7$ kJ mol^{-1}) is mainly caused by (ii), which leads to an average binding enthalpy $\Delta H(Mg–O) = -18.7/2 \approx -9$ kJ mol^{-1}. The entropy change ($\Delta S_s = -79.3$ J mol^{-1} K^{-1}) stems from (iii) (note that (i) alone implies $\Delta S = 0$) and leads to the average decrease in entropy per bonded molecule of THF of $\Delta S(THF) = -79.3/2 \approx 40$ J mol^{-1} K^{-1}.

On the basis of this simple model, the similarity of the parameters of **3**, **5**, **6**, and **8** with those of **1** can easily be understood. The closest analogy is that between **1** and **8**: neither compounds can form intramolecular coordinative bonds, so that Scheme 1 is applicable in both cases. The parameters are in good agreement ($\Delta\,\Delta H_s = 2$ kJ mol^{-1}; $\Delta\,\Delta S_s = 15$ J mol^{-1} K^{-1}!); the minor differences are within the limits of error of the experimental values, and even if real they indicate that substituent influences are of minor importance only (assumptions (2) and (4)).

For **3**, **5**, and **6**, one must assume that intramolecular coordination occurs according to Scheme 5 [6–8]. The number of chelate rings, upon going from left to right, remains the same because **3a**, **5a**, and **6a** have two intramolecular coordinative bonds which completely satisfy the tendency towards the tetra-coordination of magnesium. The resulting overall change is the binding of two additional molecules of THF ($\Delta(THF) = +2$; $\Delta(Mg–O) = +2$), just as for **1** and **8**; the thermodynamic parameters reflect this analogy.

The parameters of **4** and **7** deviate considerably from those for the other compounds investigated. This deviation indicates a completely different complexation behaviour, and is, from the intramolecular coordination point of view, most intriguing. Since both compounds belong to the same category of 2,6-disubstituted aryl-Grignards, it is remarkable that the deviation is in the opposite direction for these two compounds: strongly positive for **4** and strongly negative for **7** (Table 2). Although a rationalization of these phenomena could be based exclusively on the available thermodynamic parameters, this would be highly speculative without exact knowledge of the coordination numbers of **4** and **7**. Fortunately, suitable crystals of

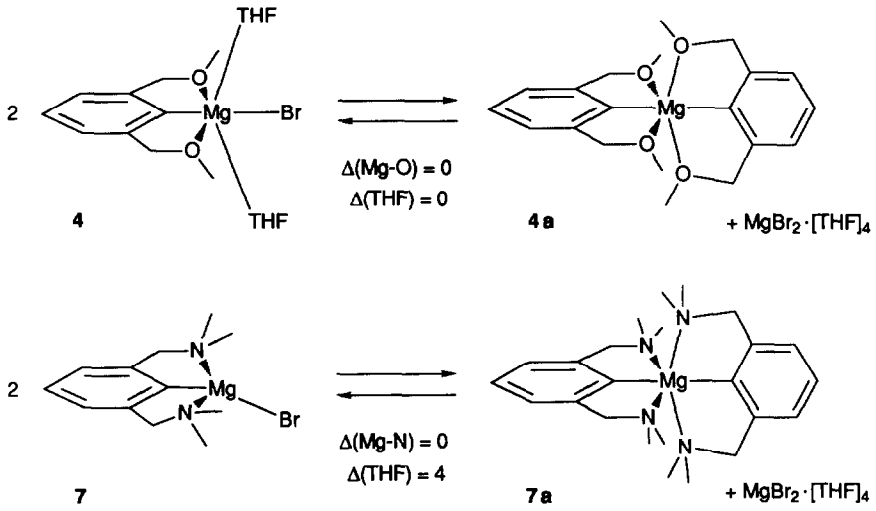

Scheme 6

4a could be isolated and were subjected to a crystal structure determination. The structure is shown in Fig. 2 and is discussed in detail in the appropriate section below. At this stage it is sufficient to note that in the solid state, **4a** is hexa-coordinate and does not contain solvent molecules. The four ether oxygens are part of an intramolecular arrangement, which reduces to a considerable extent the steric hindrance that would be involved in coordination of four separate ether molecules. This reduction in steric hindrance allows a coordination number that is unusually high for an organomagnesium compound.

As for **2a**, we assume that hexa-coordination is maintained in solution not only for **4a**, but also for **4**. Justification for this hypothesis may be derived from **2a**: the intramolecular coordination in **2a** apparently creates sufficient free space around the central magnesium atom to allow the coordination of a second molecule of THF. The coordinative unsaturation of magnesium (which strives when possible to reach a coordination number of six, as commonly found in inorganic compounds) is thus diminished by attaining the penta-coordinated state. Extrapolation of this effect to **4**, which has two intramolecular ether ligands, makes it plausible that **4**, like **4a**, is hexa-coordinate. More importantly, this hypothesis perfectly explains the deviating thermodynamic parameters for the equilibrium **4**/**4a** (Scheme 6). In the conversion of two molecules **4** into **4a** and $MgBr_2$, neither the number of coordinated molecules of THF nor the number of Mg–O bonds change. Consequently, the values of ΔH_s and ΔS_s are predicted to be zero (vide supra), and indeed, rather small values are found experimentally ($\Delta H_s = 6.8$ kJ mol^{-1}, $\Delta S_s = 23.0$ J mol^{-1} K^{-1}). Interpreting these data in a more quantitative fashion is probably extending the hypothesis too far. One can argue, however, that the thermodynamic stability of **4a** is reduced relative to that of **4** by the small bite-angle of the intramolecular ligand (C–Mg–O: 73°). While **4** has the possibility of adjusting the positions of the THF ligands to optimize its coordination geometry, **4a** is left with an imperfect octahedral coordination. The strain in the four five-membered rings of **4a** will contribute to the endothermicity of the transformation of **4** into **4a**.

The situation is completely different for the combination **7**/**7a** (Scheme 6). Penta- or hexa-coordination of **7** by the intramolecular dimethylaminomethyl ligands is impossible for two reasons. In the first place, it is well known that an amino group is a much stronger Lewis base than an ether function. While in Grignard chemistry this property seldom is effective because it is overruled by the larger size of a tertiary amine in comparison to a di-coordinated ether oxygen, steric hindrance is reduced by the amino ligand's being intramolecular in **7**. Consequently the two amino ligands in **7** will saturate the electron demand of the Lewis acidic magnesium much more effectively than the two ether oxygens of **4**. Secondly, once the two tertiary amino groups of **7** are coordinated to magnesium, the steric hindrance towards addition of extra molecules of THF will be much larger than in **4**. Thus, both for electronic and for steric reasons, **7** stays tetra-coordinate, in contrast to **4**; on the other hand, **7a** is hexa-coordinate like **4a** since all the ligands are intramolecular.

What are the consequences for the Schlenk equilibrium? Upon conversion of **7** into **7a**, four molecules of THF are needed to solvate the magnesium bromide, which is unfavourable due to the large negative entropy. On the basis of the estimate derived from the data of **1** (vide supra), a value for $\Delta S_s = 4 \times (-40) = -160$ J mol^{-1} K^{-1} can be expected, which is in good agreement with the experimental value of -175 J mol^{-1} K^{-1}. While the number of coordinate Mg–N bonds does not change, four new Mg–O bond are formed in the $MgBr_2 \cdot [THF]_4$ complex. Consequently, a value for ΔH_s of $4 \times (-9) = -36$ kJ mol^{-1} can be expected (vide supra) which is in excellent agreement with the experimental value of -33.9 kJ mol^{-1}.

The van 't Hoff-plots for **5** and **6** show an interesting effect. The initially straight lines of these plots begin to curve at lower temperatures and finally turn into a straight line with opposite slope. Although the low temperature data (second entries in Table 2) are rather inaccurate due to few data points and significant line broadening in the low temperature spectra, their evaluation yields thermodynamic

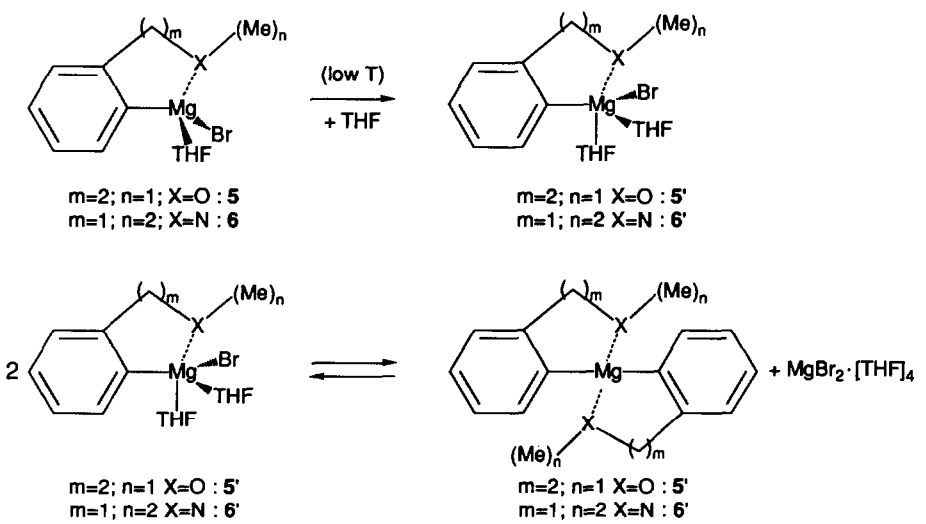

Scheme 7

parameters (**5**: $\Delta H_s = 8$ kJ mol^{-1}, $\Delta S_s = 36$ J mol^{-1} K^{-1}; **6**: $\Delta H_s = 10$ kJ mol^{-1}, $\Delta S_s = 10$ J mol^{-1} K^{-1}) which are comparable with those for **4** ($\Delta H_s = 6.8$ kJ mol^{-1}, $\Delta S_s = 23.0$ J mol^{-1} K^{-1}). We tentatively explain them as shown in Scheme 7.

In comparison with **1** and **8**, **5** and **6** have a slight bias towards higher coordination numbers because one of their ether ligands is intramolecular and hence less crowded (vide supra); addition of a second molecule of THF (i.e. the transformation **5** (or **6**) → **5′** (or **6′**)) is favoured by enthalpy (ΔH(Mg–O) = −9 kJ mol^{-1}), but disfavoured by entropy (ΔS(THF) = −40 J mol^{-1} K^{-1}). Due to the negative entropy, this transformation is favoured at lower temperatures. For **5′** and **6′** the Schlenk equilibrium involves Δ(THF) = 0 and Δ(Mg–O) = 0 just as for **4**. This interesting phenomenon merits further investigation.

Crystal structures of 2a and 4a

Crystallization from large scale preparations (see Experimental section) of Grignards **3–7** and diarylmagnesium compounds **3a–6a** was attempted from THF solutions by slow evaporation of the solvent or cooling. This technique was successful only for **2a**. For the crystallization of other compounds, concentrated THF solutions were diluted with an apolar solvent (n-hexane), and this was followed by evaporation of the solvent and cooling, but only **4a** gave crystals suitable for a structural determination.

A striking aspect of the structure of **2a** is its pseudo-trigonal bipyramidal (TBP) coordination geometry, which is rarely found in organomagnesium compounds. Only one example, MeMgBr · [THF]$_3$, has been reported so far [7]. The unexpected coordination number in **2a** clearly shows the importance of this structure determination, since initially it was assumed that upon conversion of **2** into **2a**, a simple substitution of one intermolecular magnesium–THF bond by an intramolecular ether oxygen took place (retention of tetra-coordination of the magnesium atom [6–8]). It appears, however, that the coordination number is increased from four (normal tetrahedral configuration) to five. The small intra-annular C_{ipso}–Mg–O_{intra} angles of the two six-membered chelate rings (88.2 and 88.7°; axial/equatorial angles ideally 90°) in the TBP geometry will minimize the conformational strain of the complex relative to that for a tetrahedral geometry, which would require much larger angles (approx. 109°). In this way, a higher coordination number is imposed on the magnesium atom, yielding a position to bind a second molecule of THF.

Relevant data on the geometry can be found in Table 3. The bond distances in **2a** reflect a normal TBP geometry: the axial ligands have relatively long bonds to magnesium (Mg–O(1) 2.242(4), Mg–O(3) 2.221(4) Å) while in the equatorial plane, bond lengths have normal values (Mg–C(1) 2.165(4), Mg–C(16) 2.155(4), Mg–O(2) 2.095(3) Å), which result from two opposite effects: bond extension due to a higher coordination number and bond contraction due to tighter bonding of the equatorial ligands. Bond angles show the TBP geometry to be somewhat distorted: a relatively small angle is found for O(1)–Mg–O(3) (169.6(2)°), probably due to steric interactions of the O(3) THF molecule with both aryl groups (especially the hydrogen atoms on C(2) and C(15)). The C–Mg–C angle (130.0(2)°) is somewhat expanded; this seems to be a general phenomenon and is also observed in organomagnesium compounds with tetra-coordinate magnesium atoms. The sum of the equatorial angles (C(1)–Mg–C(16) 130.0(2), C(1)–Mg–O(2) 109.9(2), C(16)–Mg–O(2)

Table 3

Bond distances (Å) and bond angles (deg) for **2a**

Mg–O(1)	2.242(4)	C(1)–C(2)	1.398(7)	C(11)–C(16)	1.416(6)
Mg–O(2)	2.095(3)	C(1)–C(6)	1.427(6)	C(12)–C(13)	1.364(8)
Mg–O(3)	2.221(4)	C(2)–C(3)	1.404(8)	C(13)–C(14)	1.388(8)
Mg–C(1)	2.165(4)	C(3)–C(4)	1.377(9)	C(14)–C(15)	1.389(7)
Mg–C(16)	2.155(4)	C(4)–C(5)	1.376(9)	C(15)–C(16)	1.408(6)
O(1)–C(8)	1.438(6)	C(5)–C(6)	1.385(7)	C(17)–C(18)	1.511(9)
O(1)–C(9)	1.438(6)	C(6)–C(7)	1.507(8)	C(18)–C(19)	1.44(1)
O(2)–C(17)	1.449(7)	C(7)–C(8)	1.499(8)	C(19)–C(20)	1.493(9)
O(2)–C(20)	1.439(7)	C(9)–C(10)	1.507(8)	C(21)–C(22)	1.404(9)
O(3)–C(21)	1.408(7)	C(10)–C(11)	1.502(7)	C(22)–C(23)	1.45(1)
O(3)–C(24)	1.434(6)	C(11)–C(12)	1.397(7)	C(23)–C(24)	1.450(9)

O(1)–Mg–O(2)	87.7(1)	C(1)–C(6)–C(5)	121.7(5)
O(1)–Mg–O(3)	169.6(2)	C(1)–C(6)–C(7)	119.7(4)
O(1)–Mg–C(1)	88.7(2)	C(5)–C(6)–C(7)	118.6(5)
O(1)–Mg–C(16)	88.2(2)	C(6)–C(7)–C(8)	113.8(5)
O(2)–Mg–O(3)	82.3(1)	O(1)–C(8)–C(7)	111.0(5)
O(2)–Mg–C(1)	109.9(2)	O(1)–C(9)–C(10)	111.3(5)
O(2)–Mg–C(16)	119.8(2)	C(9)–C(10)–C(11)	114.6(4)
O(3)–Mg–C(1)	97.6(1)	C(10)–C(11)–C(12)	118.5(4)
O(3)–Mg–C(16)	94.0(1)	C(10)–C(11)–C(16)	119.1(4)
C(1)–Mg–C(16)	130.0(2)	C(12)–C(11)–C(16)	122.4(4)
Mg–O(1)–C(8)	121.7(3)	C(11)–C(12)–C(13)	121.3(5)
Mg–O(1)–C(9)	123.5(3)	C(12)–C(13)–C(14)	118.9(5)
C(8)–O(1)–C(9)	110.5(4)	C(13)–C(14)–C(15)	119.6(5)
Mg–O(2)–C(17)	121.4(3)	C(14)–C(15)–C(16)	124.0(4)
Mg–O(2)–C(20)	129.4(4)	Mg–C(16)–C(11)	124.8(3)
C(17)–O(2)–C(20)	108.2(4)	Mg–C(16)–C(15)	120.8(3)
Mg–O(3)–C(21)	129.7(3)	C(11)–C(16)–C(15)	113.8(4)
Mg–O(3)–C(24)	121.9(3)	O(2)–C(17)–C(18)	104.3(5)
C(21)–O(3)–C(24)	108.0(4)	C(17)–C(18)–C(19)	103.8(6)
Mg–C(1)–C(2)	126.4(3)	C(18)–C(19)–C(20)	107.8(5)
Mg–C(1)–C(6)	118.2(3)	O(2)–C(20)–C(19)	106.0(5)
C(2)–C(1)–C(6)	115.0(4)	O(3)–C(21)–C(22)	109.5(5)
C(1)–C(2)–C(3)	123.3(4)	C(21)–C(22)–C(23)	106.6(6)
C(2)–C(3)–C(4)	119.0(5)	C(22)–C(23)–C(24)	107.8(5)
C(3)–C(4)–C(5)	120.1(5)	O(3)–C(24)–C(23)	106.3(5)
C(4)–C(5)–C(6)	120.8(5)		

119.8(2)°) is 360° within the limit of error, indicating the planar arrangement of the equatorial groups. In agreement with our hypothesis of conformational strain, angles between the intramolecular ether oxygen and the three equatorial ligands are smaller than 90° (O(1)–Mg–C(1) 88.7 (2), O(1)–Mg–C(16) 88.2(2), O(1)–Mg–O(2) 87.7(2)°). The corresponding angles at the other side of the complex reflect the steric interactions between the THF molecule (O(3)) and both aryl residues (O(3)–Mg–C(1) 97.6(1)°, O(3)–Mg–C(16) 94.0(1), O(3)–Mg–O(2) 82.3(1)°).

A ^{1}H NMR spectrum (in C_6D_6) of the crystals of **4a**, used for the X-ray structure determination, showed the absence of THF crystal solvent. This is a strong indication of complete intramolecular coordination, as suggested in Scheme 5, and it was confirmed by the crystal structure (Fig. 2; relevant geometric data are collected in

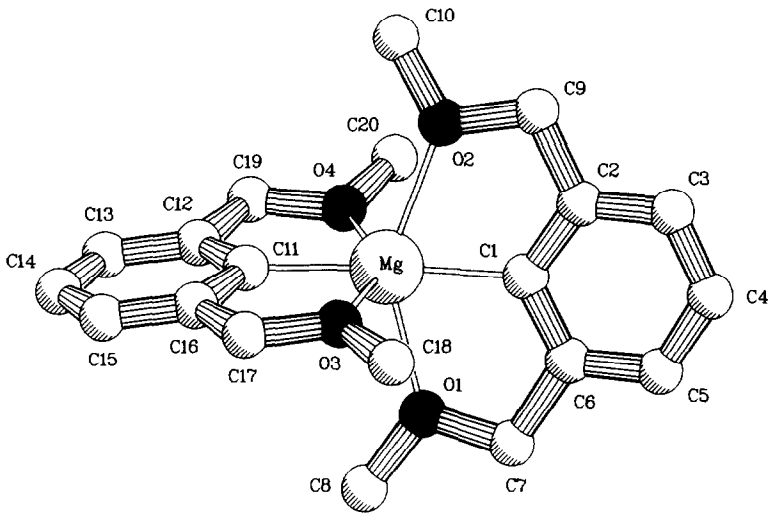

Fig. 2. PLUTON drawing of the structure of **4a**; hydrogen atoms are omitted for clarity.

Table 4): the central pseudo-octahedral magnesium atom has two opposite Mg–C bonds of surprisingly short length (Mg–C(1) 2.093(4), Mg–C(11) 2.105(4) Å), and is surrounded by four relatively weakly bonded oxygens (Mg–O(1) 2.282(3), Mg–O(2) 2.338(3), Mg–O(3), 2.327(3), Mg–O(4) 2.311(3) Å). The deviation from an ideal octahedral coordination geometry is mainly caused by strain inside the five-membered coordinative rings, resulting in small C–Mg–O angles (C(1)–Mg–O(1) 73.8(1)°, C(1)–Mg–O(2) 72.2(1)°, C(11)–Mg–O(3) 72.7(1)°, C(11)–Mg–O(4) 73.4(1)°). The C–Mg–C angle (173.4(2)°) is close to 180°, but the two aromatic rings are not quite perpendicular; their torsion angle is (75.3(2)°). The two methoxymethyl substituents of aryl group C(1–6) lie closer to the plane of their aromatic ring (0.23(1) Å) than those of aryl group C(11–16) (0.43(1) Å).

Experimental

General conditions

Aryl bromides and arylmercury compounds were synthesized under nitrogen in carefully dried reaction vessels. THF and diethyl ether were dried by distillation from $LiAlH_4$, benzene was dried by azeotropic distillation. Organic bromides were characterized by ^1H NMR spectroscopy at 90 MHz (Bruker WH-90) in $CDCl_3$ (ref. $CHCl_3 = 7.27$ ppm). Diarylmercury or diarylmagnesium compounds were characterized by ^1H NMR (250 MHz) and ^{13}C (62.89 MHz) NMR spectroscopy (Bruker WM-250) in THF-d_8 (solvent reference signals THF-d_7: 1.75 or 67.4 ppm, respectively). Gas chromatographic analysis was carried out on an Intersmat GC120, equipped with a katharometer detector (carrier gas hydrogen), or a flame ionization detector (carrier gas nitrogen). The columns used were 10% OV101 (1.5 m × 2 mm i.d., stainless steel), and 10% SE30 (1.5 m × 4 mm i.d., glass). Melting points are uncorrected. The elemental analysis of the diarylmercury compounds were carried out at the Organic Chemical Institute TNO, Zeist (The Netherlands). Concentrations of 'total base' and Mg^{2+} of organomagnesium solutions were determined after hydrolysis of a sample with known volume and titration, using acid-base or

Table 4

Bond distances (Å) and bond angles (deg) for **4a**

Mg–O(1)	2.282(3)	O(3)–C(17)	1.427(6)	C(5)–C(6)	1.391(6)
Mg–O(2)	2.338(3)	O(3)–C(18)	1.409(6)	C(6)–C(7)	1.520(6)
Mg–O(3)	2.327(3)	O(4)–C(19)	1.424(5)	C(11)–C(12)	1.393(6)
Mg–O(4)	2.311(3)	O(4)–C(20)	1.426(6)	C(11)–C(16)	1.392(5)
Mg–C(1)	2.093(4)	C(1)–C(2)	1.392(6)	C(12)–C(13)	1.399(6)
Mg–C(11)	2.105(4)	C(1)–C(6)	1.396(6)	C(12)–C(19)	1.505(6)
O(1)–C(7)	1.420(5)	C(2)–C(3)	1.392(6)	C(13)–C(14)	1.363(7)
O(1)–C(8)	1.414(6)	C(2)–C(9)	1.505(6)	C(14)–C(15)	1.368(7)
O(2)–C(9)	1.430(5)	C(3)–C(4)	1.375(8)	C(15)–C(16)	1.392(6)
O(2)–C(10)	1.414(6)	C(4)–C(5)	1.367(8)	C(16)–C(17)	1.507(6)

O(1)–Mg–O(2)	145.8(1)	Mg–C(1)–C(6)	120.6(3)
O(1)–Mg–O(3)	85.5(1)	C(2)–C(1)–C(6)	116.2(4)
O(1)–Mg–O(4)	103.7(1)	C(1)–C(2)–C(3)	122.0(4)
O(1)–Mg–C(1)	73.8(1)	C(1)–C(2)–C(9)	117.7(3)
O(1)–Mg–C(11)	103.4(1)	C(3)–C(2)–C(9)	120.3(4)
O(2)–Mg–O(3)	104.5(1)	C(2)–C(3)–C(4)	119.3(4)
O(2)–Mg–O(4)	86.3(1)	C(3)–C(4)–C(5)	121.0(5)
O(2)–Mg–C(1)	72.2(1)	C(4)–C(5)–C(6)	119.0(5)
O(2)–Mg–C(11)	110.8(1)	C(1)–C(6)–C(5)	122.5(4)
O(3)–Mg–O(4)	146.1(1)	C(1)–C(6)–C(7)	118.0(3)
O(3)–Mg–C(1)	101.1(1)	C(5)–C(6)–C(7)	119.5(4)
O(3)–Mg–C(11)	72.7(1)	O(1)–C(7)–C(6)	108.5(3)
O(4)–Mg–C(1)	112.9(1)	O(2)–C(9)–C(2)	108.8(3)
O(4)–Mg–C(11)	73.4(1)	Mg–C(11)–C(12)	120.9(3)
C(1)–Mg–C(11)	173.4(2)	Mg–C(11)–C(16)	122.2(3)
Mg–O(1)–C(7)	118.3(2)	C(12)–C(11)–C(16)	116.3(4)
Mg–O(1)–C(8)	128.9(3)	C(11)–C(12)–C(13)	121.7(4)
C(7)–O(1)–C(8)	111.4(3)	C(11)–C(12)–C(19)	117.8(3)
Mg–O(2)–C(9)	118.0(2)	C(13)–C(12)–C(19)	120.5(4)
Mg–O(2)–C(10)	128.5(3)	C(12)–C(13)–C(14)	119.6(4)
C(9)–O(2)–C(10)	112.4(3)	C(13)–C(14)–C(15)	121.0(5)
Mg–O(3)–C(17)	117.7(3)	C(14)–C(15)–C(16)	118.9(5)
Mg–O(3)–C(18)	127.9(3)	C(11)–C(16)–C(15)	122.5(4)
C(17)–O(3)–C(18)	113.6(3)	C(11)–C(16)–C(17)	117.5(4)
Mg–O(4)–C(19)	117.3(2)	C(15)–C(16)–C(17)	120.0(4)
Mg–O(4)–C(20)	129.5(3)	O(3)–C(17)–C(16)	109.5(4)
C(19)–O(4)–C(20)	111.4(3)	O(4)–C(19)–C(12)	109.6(3)
Mg–C(1)–C(2)	123.0(3)		

ethylenediamine tetraacetic acid (EDTA), respectively. The synthesis of organomagnesium reagents for NMR spectroscopy or crystallization experiments were carried out using twice sublimed magnesium. Mass spectra were recorded on a Varian CH5-DF mass spectrometer, EI 70 eV, direct inlet, or on a HP 5890 GC/5970 MS combination, EI 70 eV, and equipped with a Chrompack CP Sil 19CB 51 m/0.21 mm column. The starting materials 2-bromotoluene (Merck), 4-bromotoluene (Aldrich), 2,6-dimethylaniline (Aldrich), dimethylamine (Fluka), diphenylmercury (Merck) and mercuric bromide (Merck) were from commercial sources. The synthesis of **2a** has been described previously [5,6].

Synthesis

1-Bromo-2-bromomethylbenzene (**22**) was obtained by the photochemical bromination of 2-bromotoluene in 80% yield as previously described [10]. After repeated distillation (b.p. 127–128 °C at 16 mmHg), it solidified to a colourless low melting solid (m.p. < 35 °C). Purity was checked by ^{1}H NMR spectroscopy and GC. ^{1}H NMR (90 MHz), δ 4.64 (s, 2H, CH_2), 7.06–7.70 (m, 4H, aryl-H).

1-Bromo-2,6-bis(bromomethyl)benzene (**23**) was prepared from 1-bromo-2,6-dimethylbenzene by a method analogous to that used for **22**. After the reaction, the mixture was poured into boiling petroleum ether (b.p. 60–80 °C), slowly cooled, and kept at 5 °C for 24 h to allow crystallization. The crystals were collected, dried in vacuum over NaOH, and recrystallized from ethanol (m.p. 97–99 °C). The yield of several batches varied from 35–50%. ^{1}H NMR (90 MHz), δ 4.64 (s, 4H, CH_2), 7.18–7.56 (m, 3H, aryl-H).

1-Bromo-4-bromomethylbenzene (**24**) was obtained from 4-bromotoluene by a similar procedure. After purification by distillation (b.p. 87–90 °C at 2 mmHg), the product solidified (m.p. 59 °C, 51% yield; lit. m.p. 61 °C, 66% yield) [10]. ^{1}H NMR (90 MHz), δ 4.45 (s, 2H, CH_2), 7.27 (d, AB, $^3J = 8$ Hz, 2H, aryl-H), 7.49 (d, AB, $^3J = 8$ Hz, aryl-H).

The benzylic bromides **22–24** were converted by treatment with sodium methoxide into the corresponding methoxymethyl compounds by known procedures [11]. The crude products were purified by distillation, and characterized ^{1}H NMR spectroscopy and GC.

1-Bromo-2-methoxymethylbenzene (**9**: b.p. 95–100 °C at 9 mmHg, 90% yield; lit. b.p. 106–107 °C at 16 mmHg [12]), ^{1}H NMR (90 MHz), δ 3.50 (s, 3H, OMe), 4.54 (s, 2H, CH_2), 7.00–7.67 (m, 4H, aryl-H).

2-Bromo-1,3-bis(methoxymethyl)benzene (**10**: b.p. 115 °C at 1.5 mmHg, 78% yield), ^{1}H NMR (90 MHz), δ 3.50 (s, 6H, OMe), 4.56 (s, 4H, CH_2), 7.38 (bs, 3H, aryl-H).

1-Bromo-4-methoxymethylbenzene (**14**: b.p. 112 °C at 15 mmHg, yield 89%; lit. b.p. 110–112 °C at 8 mmHg [11]), ^{1}H NMR (90 MHz), δ 3.38 (s, 3H, OMe), 4.41 (s, 2H, CH_2), 7.20 (d, $^3J = 8$ Hz, 2H, aryl-H), 7.47 (d, $^3J = 8$ Hz, 2H, aryl-H).

1-Bromo-2-(3-oxabutyl)benzene (**11**). A suspension of KH (139 mmol) in paraffin oil was washed three times with dry diethyl ether. After addition of dry toluene (50 mL), 1-bromo-2-(2-hydroxyethyl)benzene [13] (124.4 mmol, in 50 mL dry toluene) was added dropwise. When the evolution of hydrogen gas had ceased, methyl iodide (34.2 g, 241 mmol) was added. The mixture was stirred for 24 h at room temperature, poured into water and extracted with diethyl ether. The organic layer was dried ($MgSO_4$) and filtered and the solvent evaporated. Distillation yielded (b.p. 114–116 °C at 13 mmHg; lit. b.p. 64–67 °C at 0.7 mmHg [14]) 18.2 g of the pure product as a colourless oil (68%). **11**: ^{1}H NMR (90 MHz) δ 3.01 (t, $^3J = 7$ Hz, 2H, aryl-CH_2), 3.36 (s, 3H, OMe), 3.59 (t, $^3J = 7$ Hz, 2H, CH_2-O), 6.89–7.33 (m, 3H, aryl-H), 7.40–7.62 (m, 1H, aryl-H).

1-Bromo-2-dimethylaminomethylbenzene (**12**) was prepared by adding a solution of **22** (50 g, 200 mmol) in anhydrous benzene (150 mL) dropwise during 1 h to a solution of dry dimethylamine (22.54 g, 500 mmol) in anhydrous benzene (250 mL). The reaction was carried out at a temperature of 7 °C under nitrogen. After another 50 h stirring at room temperature a white solid (Me_2NH_2Br) was filtered off under nitrogen and the solvent was removed by evaporation. A yield of 30 g **12**

(70%) was obtained as a colourless oil after vacuum distillation (b.p. 55.5 °C at 2 mmHg, lit. b.p. 104–106 °C at 9 mmHg [15]); ^{1}H NMR (90 MHz) δ 2.34 (s, 6H, Me), 3.56 (s, 2H, CH_2), 7.08–7.62 (m, 4H, aryl-H).

2-Bromo-1,3-bis(dimethylaminomethyl)benzene (**13**) [16] was prepared analogously from 34.3 g (100 mmol) of **23**. The yield after distillation (b.p. 97 °C at 0.1 mmHg) was 13.6 g (53%). ^{1}H NMR (90 MHz) δ 2.31 (s, 12H, Me), 3.54 (s, 4H, CH_2), 7.23–7.40 (m, 3H, aryl-H).

Diarylmercury compounds **15–20** were synthesized from the corresponding aryl bromides via the Grignard and the arylmercury bromide compounds (Scheme 4). Grignard reagents were prepared by dropwise adding of a solution of the corresponding bromide (80 mmol) in THF (anhydrous, 100 mL) to an excess of magnesium (100 mmol, under 20 mL of anhydrous THF), while stirring. After the reaction, the remaining magnesium was filtered off; complete conversion of the starting bromide was confirmed by hydrolysis and titration. Subsequently, a solution of mercuric bromide (31.7 g, 88 mmol, in 100 mL of anhydrous THF) was added dropwise, and the mixture was heated under reflux for one hour. After cooling, 50 mL of THF/water (1 : 1, v/v) and brine (50 mL) were added and the two resulting layers were separated. The organic layer was washed twice with brine, dried ($MgSO_4$), filtered, and evaporated to dryness, to yield the crude product. In most cases, the crude arylmercury bromides were used without further purification; those corresponding to **16** and **17** were crystallized from acetone. The arylmercury bromides were dissolved in dichloromethane and stirred with an aqueous stannate solution ($SnCl_2$/NaOH) to accomplish the reduction to the corresponding diarylmercury compounds [17]. Organic products were isolated from the reaction mixture by extraction with dichloromethane. The organic phase was dried ($MgSO_4$), filtered and the solvent evaporated to yield the crude diarylmercury compounds. The products were further dried by azeotropic distillation with benzene (100 mL) and storage in a vacuum over P_2O_5.

Bis(2-methoxymethylphenyl)mercury (**15**) was purified by sublimation (80 °C at $2 \cdot 10^{-3}$ mmHg), yield 92%. ^{1}H NMR (250 MHz) δ 3.38 (s, 6H, OMe), 4.53 (s, 4H, CH_2), 7.15 (dd, ^3J = 8 Hz, ^3J = 8 Hz, 2H, aryl-H), 7.25–7.33 (m, 4H, aryl-H), 7.47 (d, ^3J = 8 Hz, 2H, aryl-H). ^{13}C NMR (62.89 MHz) δ 57.78 (qt, ^1J(C–H) = 141 Hz, ^3J(C–H) = 4 Hz, 2C, Me), 77.66 (tqd, ^1J(C–H) = 141 Hz, ^3J(C–H) = 5 Hz, ^3J(C–H) = 5 Hz, 2C, CH_2), 127.39 (dd, ^1J(C–H) = 158 Hz, ^3J(C–H) = 7 Hz, 2C, aryl-C(4 or 5)), 127.59 (dd, ^1J(C–H) = 159 Hz, ^3J(C–H) = 8 Hz, 2C aryl-C(4 or 5)), 128.48 (d, ^1J(C–H) = 156 Hz, 2C, aryl-C(3)), 138.41 (dd, ^1J(C–H) = 159 Hz, ^3J(C–H) = 7 Hz, 2C, aryl-C(6)), 146.77 (s, 2C, aryl-C(2)), 170.56 (s, 2C aryl-C(1)). Mass spectrum, *m/z* (rel. int.) 444 ($M^{+\cdot}$,1), 414 (9), 353 (2), 323 (6), 179 (13), 91 (100). HRMS: 444.1040; $C_{16}H_{20}{}^{202}HgO_2$ calc: 444.1013. Element analysis, found: C, 42.80; H, 4.05; Hg, 45.74. $C_{16}H_{20}HgO_2$ calc.: C, 43.39; H, 4.10; Hg, 45.29%.

Bis(2,6-bis(methoxymethyl)phenyl)mercury (**16**) was purified by crystallization from diethyl ether, followed by sublimation (120–130 °C at $8 \cdot 10^{-3}$ mmHg), yield 78% (m.p. 59–60 °C). ^{1}H NMR (250 MHz) δ 3.32 (s, 12H, OMe), 4.56 (s, 8H, CH_2), 7.15 (t, ^3J = 7 Hz, 2H, aryl-H(4)), 7.29 (d, ^3J = 7 Hz, 4H, aryl-H(3,5)). ^{13}C NMR (62.89 MHz) δ 57.48 (qt, ^1J(C–H) = 141 Hz, ^3J(C–H) = 4 Hz, 4C, Me), 77.86 (tqd, ^1J(C–H) = 140 Hz, ^3J(C–H) = 5 Hz, ^3J(C–H) = 5 Hz, 4C, CH_2), 127.32 (d, ^1J(C–H) = 159 Hz, 2C, aryl-C(4)), 127.85 (ddt, ^1J(C–H) = 157 Hz, ^3J(C–H) = 7 Hz, ^3J(C–H) = 4 Hz, ^3J(C–^{199}Hg) = 85 Hz, 4C, aryl-C(3)), 147.09 (dt, ^3J(C–H) = 7 Hz, ^3J(C–H)

= 4 Hz, 4C, aryl-C(2)), 170.67 (s, 2C aryl-C(1)). Mass spectrum, *m/z* (rel. int.) 532 ($M^{+\cdot}$,2), 502 (19), 367 (11), 191 (14), 165(14), 135 (55), 134 (100), 119 (19), 105 (88), 91 (19), 77 (13), HRMS: 532.1498; $C_{20}H_{26}^{202}HgO_4$ calc: 532.1537. Element analysis, found: C, 45.23; H, 5.04; Hg, 37.79. $C_{20}H_{26}HgO_4$ calc.: C, 45.24; H, 4.94; Hg, 37.78%.

Bis(2-(3-oxabutyl)phenyl)mercury (**17**) was purified by recrystallization from diethyl ether, followed by sublimation (80–100 °C at $6 \cdot 10^{-3}$ mmHg). The yield was 59% (m.p. 62.5–63.5 °C). ^{1}H NMR (250 MHz) δ 3.03 (t, ^3J = 7 Hz, 4H, aryl-CH_2), 3.31 (s, 6H, OMe), 3.67 (t, ^3J = 7 Hz, 4H, CH_2–O), 7.11–7.41 (m, 8H, aryl-H). ^{13}C NMR (62.89 MHz) δ 41.31 (t, ^1J(C–H) = 127 Hz, ^3J(C–^{199}Hg) = 82 Hz, 2C, aryl-CH_2), 58.69 (qt, ^1J(C–H) = 140 Hz, ^3J(C–H) = 3 Hz, 2C, Me), 75.34 (tq, ^1J(C–H) = 141 Hz, ^3J(C–H) = 5 Hz, 2C, CH_2–O), 126.29 (dd, ^1J(C–H) = 158 Hz, ^3J(C–H) = 7 Hz, ^{3}3J(C–^{199}Hg) = 102 Hz, 2C, aryl-C(5)), 127.89 (dd, ^1J(C–H) = 158 Hz, ^3J(C–H) = 8 Hz, 2C, aryl-C(4)), 130.05 (ddt, ^1J(C–H) = 155 Hz, ^3J(C–H) = 6 Hz, ^3J(C–H) = 6 Hz, ^3J(C–^{199}Hg) = 76 Hz, 2C, aryl-C(3)), 137.68 (dd, ^1J(C–H) = 158 Hz, ^3J(C–H) = 7 Hz, ^2J(C–^{199}Hg) = 84 Hz, 2C, aryl-C(6)), 147.27 (s, 2C, aryl-C(2)), 172.91 (s, 2C aryl-C(1)). Mass spectrum, *m/z* (rel. int.) 472 ($M^{+\cdot}$,1) 147 (19), 135 (100), 117 (24), 105 (95), 91 (62), 77 (22). HRMS: 472.1302; $C_{18}H_{22}{}^{202}HgO_2$ calc: 472.1326. Element analysis, found: C, 45.82; H, 4.70; Hg, 42.55. $C_{18}H_{22}HgO_2$ calc.: C, 45.91; H, 4.71; Hg, 42.59%.

Bis(2-dimethylaminomethylphenyl)mercury) (**18**) was purified by sublimation (75 °C at $2 \cdot 10^{-2}$ mmHg) to yield 94% pure product as a white solid; m.p. 70–71 °C (lit. m.p. 72 °C [18]). ^{1}H NMR (250 MHz) δ 2.27 (s, 12H, Me), 3.46 (s, 4H, CH_2), 7.15–7.58 (m, 8H, aryl-H). ^{13}C NMR (62.89 MHz) δ 45.26 (qqt, ^1J(C–H) = 133 Hz, ^3J(C–H) = 5 Hz, ^3J(C–H) = 5 Hz, 4C, Me), 67.96 (thd, ^1J(C–H) = 132 Hz, ^3J(C–H) = 5 Hz, ^3J(C–H) = 5 hz, 2C, CH_2), 126.80 (dd, ^1J(C–H) = 160 Hz, ^3J(C–H) = 7 Hz, 2C, aryl-C(5)), 127.12 (dd, ^1J(C–H) = 158 Hz, ^3J(C–H) = 8 Hz, 2C aryl-C(4)), 128.98 (ddt, ^1J(C–H) = 151 Hz, ^3J(C–H) = 6 Hz, ^3J(C–H) = 6 Hz, 2C, aryl-C(3)), 138.77 (dd, ^1J(C–H) = 160 Hz, ^3J(C–H) = 7 Hz, 2C, aryl-C(6)), 147.97 (s, 2C, aryl-C(2)), 171.23 (s, 2C, aryl-C(1)). Mass spectrum, *m/z* (rel. int.) 134 (63), 132 (100), 91 (90), 58 (53), 42 (16), 31 (13), 27 (56). HRMS: 470.1661; $C_{18}H_{24}{}^{202}HgN_2$ calc: 470.1646.

Crude bis(2,6-bis(dimethylaminomethyl)phenyl)mercury (**19**) was purified by column chromatography (silicagel 60, 70-230 mesh, 2,2 × 40 cm). After elution with 200 mL of petroleum ether (40–60 °C), fractions (100 mL) were collected with an increasing percentage (10% steps) of diethyl ether. After evaporation of the eluens, the fractions containing the pure product were identified by ^{1}H NMR spectroscopy. The yield was 33 %, m.p. 40–42 °C. ^{1}H NMR (250 MHz) δ 2.20 (s, 24H, Me), 3.54 (s, 8H, CH_2), 7.20 (m, 6H, aryl-H). ^{13}C NMR (62.89 MHz) δ 45.40 (qqt, ^1J(C–H) = 133 Hz, ^3J(C–H) = 5 Hz, ^3J(C–H) = 5 Hz, 8C, Me), 68.81 (thd, ^1J(C–H) = 131 Hz, ^3J(C–H) = 5 Hz, ^3J(C–H) = 5 Hz, 4C, CH_2), 126.33 (d, ^1J(C–H) = 158 Hz, 2C, aryl-C(4)), 127.77 (ddt, ^1J(C–H) = 155 Hz, ^3J(C–H) = 8 Hz, ^3J(C–H) = 4 Hz, 4C, aryl-C(3)), 148.00 (s, 4C, aryl-C(2)), 173.23 (s, 2C, aryl-C(1)). Mass spectrum, *m/z* (rel. int.) 191 (100), 189 (10), 146 (31), 105 (40), 58 (35). HRMS: 584.2782; $C_{24}H_{38}{}^{202}HgN_4$ calc: 584.2802.

Bis(4-methoxymethylphenyl)mercury (**20**) was purified by sublimation (120–125 °C at 10^{-2} mmHg), after crystallization from methanol. Yield 80% (m.p. 132–133 °C). ^{1}H NMR (250 MHz) δ 3.32 (s, 6H, OMe), 4.41 (s, 4H, CH_2), 7.33 (d,

^3J = 8 Hz, 4H, aryl-H), 7.41 (d, ^3J = 8 Hz, 4H, aryl-H). ^{13}C NMR (62.89 MHz) δ 57.87 (qt, ^1J(C–H) = 140 Hz, ^3J(C–H) = 4 Hz, 2C, Me), 75.08 (tq, ^1J(C–H) = 140 hz, ^3J(C–H) = 5 Hz, 2C, CH_2), 127.84 (dd, ^1J(C–H) = 157 Hz, ^3J(C–H) = 4 hz, ^3J(C–^{199}Hg) = 104 Hz, 4C, aryl-C(3)), 138.03 (dd, ^1J(C–H) = 159 Hz, ^3J(C–H) = 9 Hz, ^2J(C–^{199}Hg) = 90 Hz, 4C, aryl-C(2)), 138.71 (tt, ^3J(C–H) = 7 Hz, ^3J(C–H) = 4 Hz, 2C, aryl-4(C)), 170.64 (s, 2C aryl-C(1)). Mass spectrum, *m/z* (rel. int.) 444 ($M^{+\cdot}$,20), 242 (45), 211 (37), 180 (13), 165 (12), 121 (100), 89 (46). HRMS: 444.1031; $C_{16}H_{18}{}^{202}HgO_2$ calc: 444.1013. Element analysis, found: C, 43.35; H, 4.16; Hg, 45.20. $C_{16}H_{20}HgO_2$ calc.: C, 43.39; H, 4.10; Hg, 45.29%.

Variable temperature NMR spectroscopy

Solutions of the Grignard and diarylmagnesium reagents were prepared in specially designed, fully sealed glassware (high vacuum technique) by reacting the aryl bromides **9–14** or the diarylmercury compounds **15–21** with magnesium. The reactions were carried out on a very small scale (about 50 μmol) in 500 μL THF-d_8. To ensure complete reaction, the Grignard solutions were stirred for one week; stirring for two to three weeks was used for diarylmagnesium compounds. After settling of the magnesium (amalgam) dust, the organomagnesium solution was carefully decanted into the NMR tube sealed to the glass apparatus. By means of local cooling, the remaining solvent was distilled into the NMR tube which was subsequently sealed.

The purity of each sample was checked with ^{1}H NMR spectroscopy. With **19**, no reaction took place. In all other cases, formation of the desired organomagnesium species was complete and without side products.

Diphenylmagnesium (**1a**) ^{1}H NMR (250 MHz) δ 6.89 (tt, ^3J = 7 Hz, ^4J = 2 Hz, 2H, aryl-H(4)), 6.98 (ddm, ^3J = 7 Hz, ^3J = 7 Hz, 4H, aryl-H(3)), 7.70 (dm, ^3J = 7 Hz, 4H, aryl-H(2)). ^{13}C NMR (62.89 MHz) δ 124.34 (dt, ^1J(C–H) = 155 Hz, ^3J(C–H) = 8 Hz, 2C, aryl-C(4)), 126.16 (d, ^1J(C–H) = 152 Hz, 4C, aryl-C(3)), 141.14 (ddd, ^1J(C–H) = 151 Hz, ^3J(C–H) = 12 Hz, ^3J(C–H) = 7 Hz, 4C, aryl-C(2)), 169.94 (s, 2C, aryl-C(1)).

Bis(2-methoxymethylphenyl)magnesium (**3a**) ^{1}H NMR (250 MHz) δ 3.39 (s, 6H, OMe), 4.53 (s, 4H, CH_2), 7.17 (dd, ^3J = 7 Hz, ^4J = 2 Hz, 2H, aryl-H(5)), 7.21–7.36 (m, 4H, aryl-H(3,4)), 7.49 (t, ^3J = 7 Hz, 2H, aryl-H(6)). ^{13}C NMR (62.89 MHz) δ 57.84 (qt, ^1J(C–H) = 141 Hz, ^3J(C–H) = 5 Hz, 2C, OMe), 77.60 (tqd, ^1J(C–H) = 140 Hz, ^3J(C–H) = 5 Hz, ^3J(C–H) = 5 Hz, 2C, aryl-CH_2), 127.45 (dd, ^1J(C–H) = 158 Hz, ^3J(C–H) = 7 Hz, 2C, aryl-C(4 or 5)), 127.62 (dd, ^1J(C–H) = 159 Hz, ^3J(C–H) = 8 Hz, 2C, aryl-C(4 or 5)), 128.51 (ddt, ^1J(C–H) = 156 Hz, ^3J(C–H) = 7 Hz, ^3J(C–H) = 4 Hz, 2C, aryl-C(3)), 138.44 (dd, ^1J(C–H) = 159 Hz, ^3J(C–H) = 7 Hz, 2C, aryl-C(6)), 146.74 (s, 2C, aryl-C(2)), 170.53 (s, 2C, aryl-C(1)).

Bis(2,6-bis(methoxymethyl)phenyl)magnesium (**4a**) ^{1}H NMR (250 MHz) δ 3.34 (s, 12H, OMe), 4.62 (s, 8H, CH_2), 6.77 (d, ^3J = 8 Hz, 4H, aryl-H(3,5)), 6.96 (t, ^3J = 8 Hz, 2H, aryl-H(4)). ^{13}C NMR (62.89 MHz) δ 57.99 (qt, ^1J(C–H) = 142 Hz, ^3J(C–H) = 2 Hz, 4C, OMe), 78.63 (tqd, ^1J(C–H) = 140 Hz, ^3J(C–H) = 4 Hz, ^3J(C–H) = 4 Hz, 4C, aryl-CH_2), 119.62 (dd, ^1J(C–H) = 151 Hz, ^3J(C–H) = 6 Hz, 4C, aryl-C(3)), 124.83 (d, ^1J(C–H) = 156 Hz, 2C, aryl-C(4)), 147.14 (dt, ^3J(C–H) = 7 Hz, ^2J(C–H) = 5 Hz, 4C, aryl-C(2)), 163.00 (s, 2C, aryl-C(1)).

Bis(2-(3-oxabutyl)phenyl)magnesium (**5a**) ^{1}H NMR (250 MHz) δ 2.93 (t, ^3J = 6 Hz, 4H, aryl-CH_2), 3.41 (s, 6H, OMe), 3.79 (t, ^3J = 6 Hz, 4H, CH_2–O), 6.85–6.87

(m, 6H, aryl-H), 7.62–7.66 (m, 2H, aryl-H). ^{13}C NMR (62.89 MHz) δ 59.71 (q, ^{1}J(C–H) = 142 Hz, 2C, OMe), 41.67 (t, ^{1}J(C–H) = 124 Hz, 2C, aryl-CH_2), 77.27 (tq, ^{1}J(C–H) = 142 Hz, ^{3}J(C–H) = 5 Hz, 2C, CH_2–O), 123.95 (ddt, ^{1}J(C–H) = 152 Hz, ^{3}J(C–H) = 7 Hz, ^{3}J(C–H) = 4 Hz, 2C, aryl-C(3)), 124.29 (dd, ^{1}J(C–H) = 155 Hz, ^{3}J(C–H) = 8 Hz, 2C aryl-C(4 or 5)), 125.62 (dd, ^{1}J(C–H)) = 149 Hz, ^{3}J(C–H) = 5 Hz, 2C, aryl-C(4 or 5)), 140.83 (dd, ^{1}J(C–H) = 150 Hz, ^{3}J(C–H) = 4 Hz, 2C, aryl-C(6)), 150.32 (dd, ^{3}J(C–H) = 11 Hz, ^{3}J(C–H) = 5 Hz, 2C, aryl-C(2)), 172.00 (s, 2C, aryl-C(1)).

Bis(2-dimethylaminomethylphenyl)magnesium (**6a**) ^{1}H NMR (250 MHz) δ 2.52 (s, 12H, Me), 3.57 (s, 4H, CH_2), 6.81–6.90 (m, 6H, aryl-H), 7.84–7.87 (m, 2H, aryl-H). ^{13}C NMR (62.89 MHz) δ 45.52 (qqt, ^{1}J(C–H) = 134 Hz, ^{3}J(C–H) = 5 Hz, ^{3}J(C–H) = 5 Hz, 4C, Me), 69.95 (thd, ^{1}J(C–H) = 131 Hz, ^{3}J(C–H) = 5 Hz, ^{3}J(C–H) = 5 Hz, 2C, aryl-CH_2), 124.27 (dd, ^{1}J(C–H) = 155 Hz, ^{3}J(C–H) = 8 Hz, 2C, aryl-C(5)), 124.66 (dm, ^{1}J(C–H) = 152 Hz, 2C, aryl-C(3 or 4)), 124.80 (dm, ^{1}J(C–H) = 152 Hz, 2C, aryl-C(3 or 4)), 141.48 (dm, ^{1}J(C–H) = 151 Hz, 2C, aryl-C(6)), 148.68 (s, 2C, aryl-C(2)), 171.26 (s, 2C, aryl-C(1)).

Bis(2,6-bis(dimethylaminomethyl)phenyl)magnesium (**7a**) was prepared by reacting a solution of 0.5 mmol of **7** in THF (vide supra) with a solution of 0.5 mmol of the corresponding organolithium compound [19], obtained from the lithiation of **13** with n-butyllithium [15] in THF. After evaporation of the solvent, the resulting oil was dissolved in toluene and filtered to remove the lithium bromide, formed in the reaction. After removal of the toluene by evacuation, the remaining oil was taken up in THF-d_8 and divided over two NMR tubes which, subsequently, were melted off. ^{1}H NMR (90 MHz) δ 6.85 (m, 6H, aryl), δ 3.45 (s, 8H, CH_2), δ 2.28 (s, 24, CH_3). One of the NMR tubes contained $\pm$0.25 mmol anhydrous magnesium bromide which yielded the corresponding Grignard reagent. This experiment enabled the identification of the product which was not possible by quenching and titration because the starting materials would give the same results as the expected product. The peaks in the spectra of both tubes matched with those of the variable temperature experiments.

Bis(4-methoxymethylphenyl)magnesium (**8a**) ^{1}H NMR (250 MHz) δ 3.27 (s, 6H, OMe), 4.32 (s, 4H, CH_2), 7.02 (d, ^{3}J = 8 Hz, 4H, aryl-H(3,5)), 7.73 (d, ^{3}J = 8 Hz, 4H, aryl-H(2,6)). ^{13}C NMR (62.89 MHz) δ 57.37 (qt, ^{1}J(C–H) = 140 Hz, ^{3}J(C–H) = 5 Hz, 2C, OMe), 76.43 (tq, ^{1}J(C–H) = 139 Hz, ^{3}J(C–H) = 5 Hz, 2C, aryl-CH_2), 126.05 (dt, ^{1}J(C–H) = 151 Hz, ^{3}J(C–H) = 4 Hz, 4C, aryl-C(3)), 134.03 (tt, ^{3}J(C–H) = 7 Hz, ^{3}J(C–H) = 4 Hz, 2C, aryl-C(4)), 140.97 (dd, ^{1}J(C–H) = 151 Hz, ^{3}J(C–H) = 12 Hz, 4C, aryl-C(2)), 169.22 (s, 2C, aryl-C(1)).

Prior to the variable temperature NMR measurements, the samples were kept overnight at $-80\,^{\circ}$C to ascertain that no crystallization would occur during the low temperature measurements. ^{1}H NMR spectra were measured for all the Grignard solutions. In the spectra of **3–7**, most signals of the Grignard and diarylmagnesium species were discernible but only those of the methyl groups (sharp singlets) were sufficiently separated. Identification was possible by comparing these spectra with those of the diarylmagnesium compounds recorded under identical conditions. For each compound, spectra were recorded over a broad temperature range. Determination of the signal areas was performed by electronic integration.

For **1** and **8**, suitable signals were not found in the ^{1}H NMR spectra and so ^{13}C NMR spectroscopy was necessary, although this technique is more time consuming

due to the large number of pulses (7000–10000) required. Peak areas were determined from expanded plots by cutting and weighing. Values of K were calculated for the different carbon atoms from a single spectrum and a mean value was determined. The signals of the quaternary carbons were discarded because of their low intensities, caused by slow relaxation.

The temperature ranges and the ln K values derived from the NMR spectra of each compound, are listed in Table 1.

Large scale preparations of organomagnesium compounds

To obtain larger quantities of the Grignards reagents **3–7** and diarylmagnesium compounds **3a–6a** for crystallization experiments, reactions (typically 5–10 mmol scale) of aryl bromides **9–13** or diarylmercury compounds **15–18** with magnesium were performed. From the NMR experiments, it was known that no side products were formed in these reactions. Complete conversion of the starting material into the desired product was further confirmed by hydrolysis and titration of 'total base' (HCl) and Mg^{2+} (EDTA); the expected ratios for Grignards (1 : 1) and diorganylmagnesiums (2 : 1) were found. To obtain solutions of high purity, the reactions were carried out in fully sealed glassware using high vacuum techniques, thus preventing hydrolysis or oxidation.

In the Grignard reactions the bromides (10 mmol) were added in small portions to magnesium (twice sublimed, 20 mmol, 0.5 g) in THF (100 mL) and stirred over a period of about 30 hours. After settling of the magnesium dust, the clear Grignard solution was decanted into a second vessel.

Diarylmagnesium compounds were prepared by stirring the corresponding diarylmercury compounds (10 mmol) with a large excess of magnesium (100 mmol, 2.4 g) in THF (100 mL) during a period of 1–2 weeks. After settling of the magnesium amalgam, the organomagnesium solutions were decanted into a second vessel.

Crystallizations

Crystals of **2a** were obtained by the slow evaporation from a THF solution at room temperature. After decantation of the mother liquor, the dry crystals were isolated and partially used for characterization by ^{1}H NMR spectroscopy. Their solubility in THF-d_8 proved to be low, which made the determination of the amount of crystal solvent (THF) inaccurate. The remaining crystals were introduced into a nitrogen filled glovebox and mounted in Lindemann capillaries. In the glovebox, the crystals disintegrated within several days due to loss of crystal solvent. The remaining solid was hydrolyzed and titrated, to confirm their 'total base' to Mg^{2+} ratio of 2 : 1. The mother liquor of the crystallization of **2a** was quenched with D_2O, water was added, and the organic material was isolated by extraction with CH_2Cl_2. The organic phase was dried ($MgSO_4$), filtered, and evaporated to dryness. The colourless residue was characterized by ^{1}H NMR spectroscopy and GCMS, and proved to be pure, [2-D]2,2′-bis(phenyl)diethyl ether). ^{1}H NMR ($CDCl_3$, 250 MHz, ref. $CHCl_3$ = 7.27 ppm), δ 2.90 (t, ^3J = 7 Hz, 4H, CH_2–O), 3.67 (t, ^3J = 7 Hz, 4H, aryl-CH_2), 7.19–7.32 (m, 8H, aryl-H). GCMS mass spectrum, m/z (rel. intensity) 228 (1) $M^{+\cdot}$, 136 (9), 106 (100), 92 (17).

2: ^{1}H NMR (THF-d_8, 250 MHz, ref. THF-d_7 = 1.80 ppm), δ 2.89 (t, ^3J = 5 Hz, 4H, aryl-CH_2), 3.78 (t, ^3J = 5Hz, 4H, CH_2–O), 6.75–6.81 (m, 6H, aryl-H), 7.67 (dm,

$^3J = 6$ Hz, 2H). In this spectrum, the ratio of THF-H_8: **2a** was larger than 4. ^{1}H NMR (C_6D_6, 250 MHz, ref. $C_6D_5H = 7.30$ ppm), δ 2.92 (m, broad, 4H, CH_2–O), 3.48 (m, broad, 4H, aryl-CH_2), 7.50 (dd, $^3J = 7$ Hz, $^3J = 7$ Hz, 2H, aryl-H), 7.58 (dd, $^3J = 7$ Hz, $^3J = 7$ Hz, 2H, aryl-H), 8.41 (d, $^3J = 7$ Hz, 2H, aryl-H). Because of the low solubility of **2a** in benzene, the solvent signals in this spectrum were very intense. One aryl-H signal was not detected; it was probably obscured by the C_6D_5H signal.

Initially, crystallization of **3**–**7** and **3a**–**6a** was attempted by distilling off part of the THF and then cooling the solution to −20 and −80 °C. In some cases crystallization did occur, but the solid separated as a compact lump. Therefore, dilution of the THF solutions with an apolar solvent was tried. The organomagnesium solutions were divided into smaller samples (1 mmol in 10 mL THF). Each sample was concentrated by distilling off most of the THF (7–9 mL) and n-hexane (about 10 mL) was added to obtain a solution saturated at room temperature. Upon cooling (+5 to −20 °C), crystals suitable for X-ray structure determination were obtained from **4a**. Only low quality crystals were obtained in the other cases.

Table 5a

Crystal data and details of the structure determination of **2a**

(a) *Crystal data*	
Formula	$C_{24}H_{32}O_3Mg$
Mol. wt.	392.82
Crystal system	monoclinic
Space group	$P2_1/a$ (non-standard setting of No. 14)
a, b, c (Å)	9.262(6), 19.399(4), 12.490(3)
β (°)	90.40(4)
V (Å^3)	2244(2)
Z	4
D_{calc} (g cm^{-3})	1.163
$F(000)$	848
μ (cm^{-1})	8.1
Crystal size (mm)	0.20×0.20×1.00
(b) *Data collection*	
Temperature (K)	294
θ_{min}, θ_{max} (°)	2.28, 70.0
Radiation	Cu-K_α (Ni-filtered), 1.54184 Å
Scan type	$\omega/2\theta$
$\Delta\omega$(°)	0.80 + 0.15 tan θ
Hor. and vert. aperture (mm)	4.0, 5.0
Dist. cryst. to detector (mm)	173
Reference reflections	1 −2 −2, −1 1 0
Data set	h 0:11; k 0:23; l −15:15
Total data	4670
Total unique data	4242
Observed data	2179 [$I > 2.5\sigma(I)$]
(c) *Refinement*	
No. of refined parameters	254
Weighting scheme	$w = 1.0/[\sigma^2(F) + 0.000311F^2]$
Final R, R_w, S	0.067, 0.075, 1.09
$(\Delta/\sigma)_{av}$ in final cycle	0.016
min. and max. resd. dens. e/Å^3	−0.23, 0.24

Table 5b

Crystal data and details of the structure determination of **4a**

(a) *Crystal data*	
Formula	$C_{20}H_{26}O_4Mg$
Mol. wt.	354.73
Crystal system	monoclinic
Space group	$P2_1/n$ (non-standard setting of No. 14)
a, b, c (Å)	12.660(3), 12.413(2), 12.892(3)
β (°)	90.76(2)
V (Å^3)	2025.8(7)
Z	4
D_{calc} (g cm^{-3})	1.163
$F(000)$	760
μ (cm^{-1})	8.9
Crystal size (mm)	0.20×0.20×0.90
(b) *Data collection*	
Temperature (K)	294
$\theta_{min}, \theta_{max}$ (°)	3.43, 70.0
Radiation	Cu-K_α (Ni-filtered), 1.54184 Å
Scan type	$\omega/2\theta$
$\Delta\omega$(°)	0.30+0.15 tan θ
Hor. and vert. aperture (mm)	2.0, 6.0
Dist. cryst. to detector (mm)	173
Reference reflections	2 0 0, 0 2 0
Data set	h −15:15; k 0:15; l 0:15
Total data	4218
Total unique data	3836
Observed data	1732 [$I > 2.5\sigma(I)$]
(c) *Refinement*	
No. of refined parameters	239
Weighting scheme	$w = 1.0/[\sigma^2(F) + 0.000531F^2]$
Final R, R_w, S	0.053, 0.064, 0.83
$(\Delta/\sigma)_{av}$ in final cycle	0.019
min. and max. resd. dens. e/Å^3	−0.16, 0.15

Some dry crystals of **4a** were used for characterization by ^{1}H NMR spectroscopy in C_6D_6, and this indicated that no THF was present. The mother liquor of **4a** was quenched with D_2O, water was added, the organic layer separated and the water phase extracted with CH_2Cl_2. The combined organic phases were dried ($MgSO_4$), filtered and evaporated to dryness. The residue (colourless oil) was characterized by ^{1}H NMR spectroscopy as [2-D]1,3-bis(methoxymethyl)benzene (> 90% pure).

4a: ^{1}H NMR (C_6D_6, 250 MHz, ref. C_6D_5H = 7.30 ppm), δ 3.16 (s, 12H, OMe), 4.61 (s, 8H, aryl-CH_2), 7.16 (d, ^3J = 7 Hz, 4H, aryl-H(3,5)), 7.51 (t, ^3J = 7 Hz, 2H, aryl-H(4)). [2-D]1,3-bis(methoxymethyl)benzene: ^{1}H NMR ($CDCl_3$, 250 MHz, ref. $CHCl_3$ = 7.27 ppm), δ 3.41 (s, 6H, OMe), 4.48 (s, 4H, aryl-CH_2), 7.25–7.36 (m, 3 H, aryl-H).

Structure determination and refinement of **2a**

Crystal data and numerical details of the structure determination are given in Table 5. A colourless rod shaped crystal was mounted under nitrogen in a Linde-

Table 6

Final coordinates and equivalent isotropic thermal parameters and their e.s.d. in parentheses for **2a**

Atom	x	y	z	U_{eq} [a] (Å^2)
Mg	−0.0950(2)	0.40423(7)	0.2410(1)	0.0582(5)
O(1)	0.0036(3)	0.2994(2)	0.2226(3)	0.071(1)
O(2)	0.1150(3)	0.4439(2)	0.2505(3)	0.076(1)
O(3)	−0.1532(4)	0.5151(2)	0.2513(2)	0.077(1)
C(1)	−0.1673(5)	0.3740(2)	0.3987(3)	0.060(2)
C(2)	−0.2998(6)	0.3905(2)	0.4452(4)	0.070(2)
C(3)	−0.3437(6)	0.3651(3)	0.5451(5)	0.084(3)
C(4)	−0.2535(8)	0.3211(3)	0.6004(4)	0.097(3)
C(5)	−0.1235(7)	0.3017(3)	0.5570(4)	0.087(2)
C(6)	−0.0806(6)	0.3266(2)	0.4583(4)	0.067(2)
C(7)	0.0594(6)	0.3010(3)	0.4122(4)	0.089(2)
C(8)	0.0408(6)	0.2576(3)	0.3138(4)	0.092(3)
C(9)	−0.0161(6)	0.2571(3)	0.1291(4)	0.086(2)
C(10)	−0.0183(6)	0.3000(3)	0.0285(4)	0.079(2)
C(11)	−0.1551(5)	0.3400(2)	0.0105(4)	0.063(2)
C(12)	−0.2364(6)	0.3267(3)	−0.0818(4)	0.078(2)
C(13)	−0.3616(7)	0.3614(3)	−0.1027(4)	0.087(3)
C(14)	−0.4085(6)	0.4105(3)	−0.0300(4)	0.082(2)
C(15)	−0.3262(5)	0.4243(2)	0.0609(3)	0.068(2)
C(16)	−0.1965(5)	0.3901(2)	0.0868(3)	0.059(2)
C(17)	0.1645(6)	0.4820(3)	0.3436(5)	0.101(3)
C(18)	0.3201(7)	0.4602(3)	0.3578(6)	0.113(3)
C(19)	0.3678(7)	0.4468(4)	0.2502(5)	0.124(3)
C(20)	0.2377(7)	0.4300(4)	0.1839(5)	0.115(3)
C(21)	−0.2128(8)	0.5524(3)	0.3370(5)	0.122(3)
C(22)	−0.2452(8)	0.6197(3)	0.3033(6)	0.125(3)
C(23)	−0.1753(9)	0.6291(3)	0.2010(6)	0.138(4)
C(24)	−0.1158(7)	0.5632(3)	0.1689(4)	0.095(3)

[a] $U_{eq} = 1/3$ of the trace of the orthogonalised U matrix.

mann glass capillary and transferred to an Enraf-Nonius CAD4F diffractometer for data collection. Unit cell parameters were determined from a least squares treatment of the SET4 setting angles of 22 reflections and were checked for the presence of higher lattice symmetry [20]. Data were corrected for Lp and for a small linear decay (3.0%) of the intensities during the 98 h of X-ray exposure time but not for absorption. Standard deviations as obtained by counting statistics were increased according to an analysis of the excess variance of the reference reflections: $\sigma^2(I) = \sigma^2_{CS}(I) + (0.017\ I)^2$ [21]. The structure was solved by direct methods (SHELXS86; [22]), and the solution with the best figures of merit revealed all the non-H atoms. Refinement on F was carried out by full-matrix least-squares techniques. H-atoms were introduced on calculated positions (C–H = 0.98 Å) and included in the refinement riding on their carrier atoms. All non-hydrogen atoms were refined with anisotropic thermal parameters, H-atoms were refined with one common isotropic thermal parameter ($U = 0.141(5)$ Å^2). Weights were introduced in the final refinement cycles, convergence was reached at $R = 0.067$. Final atomic coordinates and equivalent isotropic thermal parameters are listed in Table 6.

Table 7

Final coordinates and equivalent isotropic thermal parameters and their e.s.d. in parentheses for **4a**

Atom	x	y	z	U_{eq} [a] (Å^2)
Mg	−0.0834(1)	0.2446(1)	0.0899(1)	0.0719(5)
O(1)	0.0578(2)	0.1311(2)	0.0779(2)	0.084(1)
O(2)	−0.2257(2)	0.3241(2)	0.0015(2)	0.081(1)
O(3)	0.0419(2)	0.3812(2)	0.1038(2)	0.089(1)
O(4)	−0.2082(2)	0.1432(2)	0.1754(2)	0.076(1)
C(1)	−0.0715(3)	0.2041(3)	−0.0671(3)	0.065(2)
C(2)	−0.1428(3)	0.2399(4)	−0.1426(3)	0.072(2)
C(3)	−0.1301(4)	0.2169(4)	−0.2474(3)	0.096(2)
C(4)	−0.0441(5)	0.1577(5)	−0.2778(4)	0.118(3)
C(5)	0.0285(4)	0.1210(4)	−0.2068(4)	0.100(2)
C(6)	0.0143(3)	0.1444(4)	−0.1024(3)	0.071(2)
C(7)	0.0935(3)	0.1026(4)	−0.0224(3)	0.081(2)
C(8)	0.1313(4)	0.1002(5)	0.1559(4)	0.117(3)
C(9)	−0.2367(3)	0.3040(4)	−0.1073(3)	0.079(2)
C(10)	−0.3161(4)	0.3741(5)	0.0432(4)	0.109(2)
C(11)	−0.0784(3)	0.2941(3)	0.2460(3)	0.067(2)
C(12)	−0.1388(3)	0.2422(4)	0.3204(3)	0.069(2)
C(13)	−0.1257(4)	0.2636(4)	0.4263(3)	0.082(2)
C(14)	−0.0526(4)	0.3375(5)	0.4582(4)	0.091(2)
C(15)	0.0088(4)	0.3906(4)	0.3882(4)	0.082(2)
C(16)	−0.0045(3)	0.3682(3)	0.2830(3)	0.071(2)
C(17)	0.0630(4)	0.4247(4)	0.2044(4)	0.093(2)
C(18)	0.1128(4)	0.4168(4)	0.0278(4)	0.109(2)
C(19)	−0.2217(3)	0.1638(4)	0.2831(3)	0.082(2)
C(20)	−0.2927(4)	0.0800(4)	0.1339(4)	0.098(2)

[a] U_{eq} = 1/3 of the trace of the orthogonalized U matrix.

Structure determination and refinement of ***4a***

Crystal data and numerical details of the structure determination are given in Table 5. A colourless rod shaped crystal was mounted under nitrogen in a Lindemann glass capillary and transferred to an Enraf-Nonius CAD4F diffractometer for data collection. Unit cell parameters were determined from a least-squares treatment of the setting angles of 12 reflections with $8.5 < \theta < 15.5°$. The unit cell parameters were checked for the presence of higher lattice symmetry. Data were corrected for Lp, for a small linear decay (2.3%) of the intensities during the 65 h of X-ray exposure time and for absorption (DIFABS, [23]; correction range: 0.85–1.28). Standard deviations as obtained by counting statistics were increased according to an analysis of the excess variance of the reference reflections: $\sigma^2(I) = \sigma_{CS}^2(I) + (0.005\ I)^2$ [21]. The structure was solved by direct methods (SHELXS86); the solution with the best figures of merit revealed all non-H atoms and subsequent difference Fourier synthesis. Refinement on F was carried out by full-matrix least-squares techniques. H-Atoms were introduced on calculated positions (C–H = 0.98 Å) and included in the refinement riding on their carrier atoms. All non-hydrogen atoms were refined with anisotropic thermal parameters, H-atoms were refined with one common isotropic thermal parameter (U = 0.120(4) Å^2). Weights were introduced in the final refinements cycles, convergence was reached at R = 0.053. Final atomic coordinates and equivalent thermal parameters are listed in Table 7.

For both structure determinations, neutral atom scattering factors were taken

from [24] and corrected for anomalous dispersion [25]. All calculations were performed with SHELX76 [26] and the EUCLID package [27] (geometrical calculations and illustrations) on a MICROVAX cluster.

Supplementary material available. Anisotropic thermal parameters, H-atom parameters, lists of bond lengths, band angles, and lists of observed and calculated structure factor amplitudes for **2a** and **4a** (61 pages) are available form A.L.S.

Acknowledgements

G. Schat is thanked for the preparation of some of the organomagnesium compounds and for furnishing the large quantities of extremely dry solvents required for most experiments. X-Ray data were kindly collected by A.J.M. Duisenberg. This work was supported in part (P.R.M., A.V., W.J.J.S., A.L.S.) by the Netherlands Foundation for Chemical Research (SON) with financial aid from the Netherlands Organization for Scientific Research (NWO).

References

1 W.E. Lindsell, in G. Wilkinson, F.G.A. Stone and E.W. Abel (Eds.), Comprehensive Organometallic Chemistry, Pergamon Press, Oxford, 1982, p. 155.
2 M.B. Smith and W.E. Becker, Tetrahedron, 22 (1966) 3027.
3 M.B. Smith and W.E. Becker, Tetrahedron, 23 (1967) 4215.
4 D.F. Evans and G.V. Fazakerley, J. Chem. Soc. A, (1971) 184.
5 F.J.M. Freijee, G. van der Wal, G. Schat, O.S. Akkerman and F. Bickelhaupt, J. Organomet. Chem., 240 (1982) 229.
6 F.J.M. Freijee, Thesis Vrije Universiteit, Amsterdam, 1981.
7 M. Vallino, J. Organomet. Chem., 20 (1969) 1.
8 A. Villena, Thesis Vrije Universiteit, Amsterdam, 1986.
9 F.A. Schröder, Chem. Ber., 102 (1969) 2035, and references cited; R. Sarma, F. Ramirez, B. McKeever, Y. Fen Chaw, J.F. Marecek, D. Nierman and T.M. McCaffrey, J. Am. Chem. Soc., 99 (1977) 5289.
10 A. Roedig, in N. Kreutzkamp, H. Meerwein, A. Roedig and R. Stroh (Eds.), Methoden der Organische Chemie (Houben Weyl), Thieme Verlag, Stuttgart, 4. Aufl., Band 5/4, 1960, p. 339.
11 J.F. Sirks, Recl. Trav. Chim., Pays Bas, 65 (1946) 850.
12 F.G. Holliman and F.G. Mann, J. Chem. Soc., (1947) 1634.
13 H. Gilman and O.L. Marrs, J. Org. Chem., 30 (1965) 325.
14 F.G. Mann and I.T. Millar, J. Chem. Soc., (1951) 2205.
15 F.N. Jones and C.R. Hauser, J. Org. Chem., 63 (1962) 4389.
16 D.M. Grove, G. van Koten, H.J.C. Ubbels, R. Zoet and A.L. Spek, Organometallics, 3 (1984) 1003.
17 H. Sawatzky and G.F. Wright, Can. J. Chem., 36 (1958) 1555.
18 A.F.M.J. van der Ploeg, C.E.M. van der Kolk and G. van Koten, J. Organomet. Chem., 212 (1981) 283.
19 C.G. Screttas and M. Micha Screttas, J. Organomet. Chem., 292 (1985) 325.
20 A.L. Spek, J. Appl. Crystallogr., 21 (1988) 578.
21 L.E. McCandlish, G.H. Stout and L.C. Andrews, Acta Crystallogr., Sect. A, 31 (1975) 245.
22 G.M. Sheldrick, SHELXS86. Program for crystal structure determination. University of Göttingen, Federal Republic of Germany, 1986.
23 N. Walker and D. Stuart, Acta Crystallogr., Sect. A, 39 (1983) 158.
24 D.T. Cromer and J.B. Mann, Acta Crystallogr., Sect. A, 24 (1968) 321.
25 D.T. Cromer and D. Liberman, J. Chem. Phys., 53 (1970) 1891.
26 G.M. Sheldrick, SHELX76. Crystal structure analysis package. University of Cambridge, England, 1976.
27 A.L. Spek, The EUCLID package in D. Sayre (Ed.), Computational Crystallography, Clarendon Press, Oxford, 1982.